HTML ABSTRACT + LINKS

Visualization of second-order nonlinear layer in thermally poled fused silica glass

Honglin An[a] and Simon Fleming
Optical Fibre Technology Centre, Australian Photonics CRC, University of Sydney, 206 National Innovation Centre, Australian Technology Park, Eveleigh NSW 1430, Australia

Guy Cox
Electron Microscope Unit, University of Sydney, NSW 2006, Australia

(Received 28 June 2004; accepted 19 October 2004)

Second-harmonic microscopy has been applied to characterize the second-order nonlinear layer in fused silica plates thermally poled at 280 °C and 3.5 kV for different time intervals. The nonlinear layer is found only under the anode surface and to be ~5 μm deep under the anode for a poling time of 30 min. Progression of this layer into the bulk glass with poling time is also characterized. © *2004 American Institute of Physics*. [DOI: 10.1063/1.1835554]

Silica glass has widespread applications in modern technology, especially in optical communications, due to its excellent optical properties. But, silica glass is an amorphous and isotropic material, and, therefore, does not possess any second-order nonlinearity (SON). In 1991, however, Myers, Mukherjee, and Brueck obtained a SON of ~1 pm/V in thermally poled fused silica.[1] This result has excited intense research interest and opened up the prospect of realizing second-harmonic (SH) generation, linear electro-optic (EO) modulation and optical switching in silica optical fibers and planar waveguides. Since then, intensive effort has been put into this research direction, and now large EO coefficients have also been obtained in optical fibers and Ge-doped silica planar waveguides.[2–4] Despite these technology advances, the thermal poling mechanism is still not fully understood. Experimental results have indicated that the induced optical nonlinearity is confined to a very thin layer (a few microns), often called the depletion layer, near the anode surface. Careful characterization of this SON layer can provide important insight towards understanding the thermal poling mechanism, and many researchers around the world have studied this. The most commonly adopted method is to etch the thermally poled silica with HF.[5,6] Alley and Brueck viewed the etched samples with atomic force microscopy, and found a peaked ridge, corresponding to a slower etching rate, ~12 μm below the anode surface for the poling time of 30 min.[5] Margulis and Laurell used an interferometer to monitor the HF etching rates continuously and found the depletion layer was 2–5.5 μm deep under the anode.[6] This interferometric method was further developed to reconstruct the SON layer created inside the glass.[7] However, the drawback to this HF etching method is that it cannot distinguish between contributions to the HF etching rate change from changes of electric field and charge densities, which are both present in the depletion layer. It also destroys the SON layer by etching away all the ions under the anode surface and therefore does not represent the original SON distribution very well.

In this letter, we report the nondestructive characterization of the SON layer in thermally poled fused silica glass with SH microscopy. SH microscopy has been successfully used for investigating periodically poled ferroelectric crystals,[8] domain structures in magnetic garnet films,[9] and thermally poled synthetic silica planar waveguides,[4,10] but has not been applied to thermally poled bulk fused silica yet.

Thermal poling was performed in the open air on 1-mm-thick fused silica disks with both surfaces polished. The samples were placed on the top surface of a grounded 280 °C aluminum heater, and a copper block of a diameter of about 8 mm, serving as the anode, was placed on top of the samples. Then a dc voltage of 3.5 kV was applied across the electrodes for different time intervals. Finally the heater was switched off and the samples were allowed to cool down to room temperature before switching off the electric field.

After being thermally poled, the sample was affixed with adhesive on each side of the poled region to a piece of silicon wafer for support and protection, and then cut parallel to the direction of the applied electric field to expose the cross section of the poled silica disk. The surface of the cut sample was further polished to optical finish for SH microscopy observation.

The SH microscopy was conducted with an inverted Leica DMIRBE microscope equipped with a Leica TCS2MP confocal system and coherent Verdi-Mira tunable pulsed titanium sapphire laser. An excitation wavelength of 830 nm was used, with pulses in the 100–200 fs range. The wavelength was checked with a Rees spectrum analyzer. The microscope is also equipped with dual photomultiplier transmitted light detectors, with a 505 DCLP dichroic mirror dividing the detectable spectrum (380–680 nm) at 505 nm between the two channels. The shorter wavelength channel (channel 2) was fitted with a 415/10 narrow bandpass filter to receive only the second harmonic and reject any two-photon excited fluorescence. The longer wavelength channel (channel 1) was fitted with a 650SP, thus detecting the range from 505 to 650 nm. This channel will therefore receive two-photon fluorescence over a wide range; we also used it to detect a transmitted nonconfocal image using the 543 nm green helium–neon laser. This can be acquired simultaneously with the SH image. A x20 numerical aperture (NA) 0.5 plan-fluorite objective was used, with a dry/oil-immersion NA 0.93/1.4 condenser used dry. To obtain maximum SH signal, the sample was placed on the specimen stage in such a position that the

[a]author to whom correspondence should be addressed; electronic mail: h.an@oftc.usyd.edu.au

 © 2004 American Institute of Physics
Downloaded 12 Dec 2004 to 129.78.64.101. Redistribution subject to AIP license or copyright, see http://apl.aip.org/apl/copyright.jsp

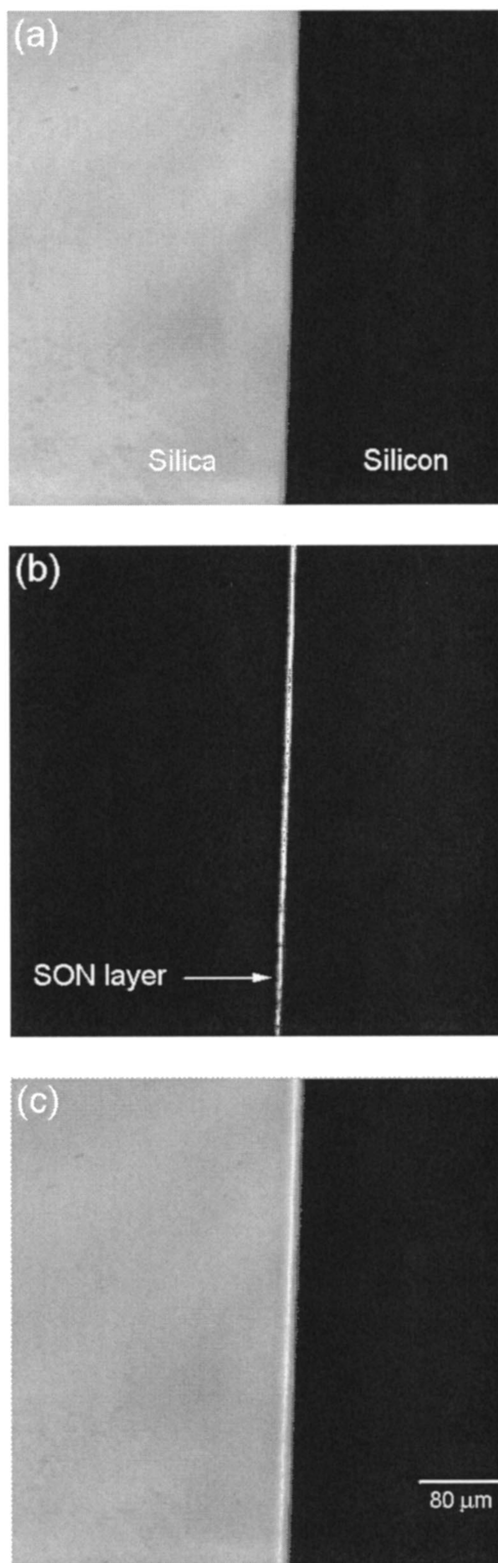

FIG. 1. SH micrographs of a fused silica thermally poled at 3.5 kV and 280 °C for 30 min. (a) Channel 1 image; (b) channel 2 image; (c) overlay image from (a) and (b).

poling direction was parallel with the polarization direction of the excitation light.

A typical result from the sample thermally poled for 30 min is shown in Fig. 1. The channel 1 image shown in Fig. 1(a) shows the area where the SH microscopy was performed and the interface between the anode surface and the glued silicon wafer can be clearly seen. The SH signal from channel 2 is shown in Fig. 1(b). A bright narrow line can be seen just under the anode surface, corresponding to a well-defined SON spatial distribution. Some discontinuity along the line could be observed, believed to be mainly due to the inhomogeneities in the fused silica. An overlay image of Figs. 1(a) and 1(b) is shown in Fig. 1(c), in which the scale bar applies also to Figs. 1(a) and 1(b).

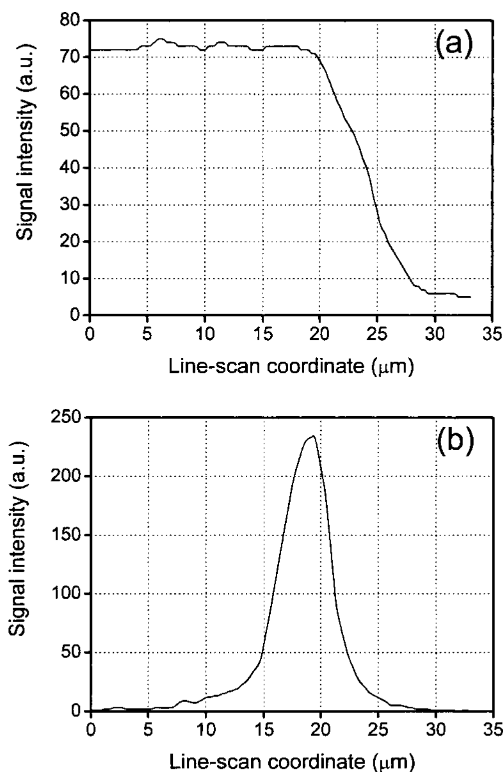

FIG. 2. Line-scan SH micrographs across the SON layer. (a) Channel 1 image; (b) channel 2 image.

In order to characterize the SON profile, we performed a line scan across the SON layer. The analysis results from both channels are shown in Fig. 2. In Fig. 2(a), as the silicon wafer is not transparent and blocked the transmission light, we can see a step in the transmission intensity and could locate the position of the interface between the anode surface and the silicon wafer fairly well. The spatial distribution of the SH signal is shown in Fig. 2(b). Since $P(2\omega) \propto P^2(\omega)d^2$, where d is the SON coefficient, the SON profile can be obtained from the square root of the measured SH signal profile. The calculated SON profile is shown in Fig. 3. The full width at half maximum (FWHM) of this profile was found to

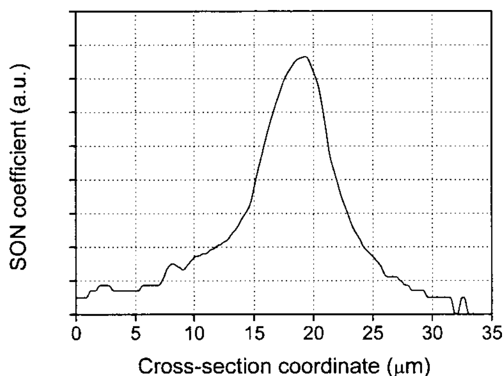

FIG. 3. Spatial distribution of the SON layer.

Downloaded 12 Dec 2004 to 129.78.64.101. Redistribution subject to AIP license or copyright, see http://apl.aip.org/apl/copyright.jsp

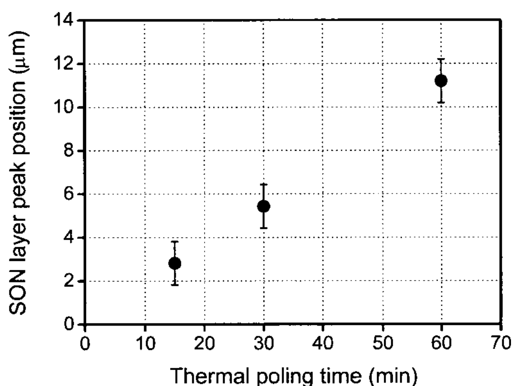

FIG. 4. Evolution of the SON layer with poling time.

be ~7 μm. By obtaining the knowledge of the interface position from Fig. 2(a), we further determined that the peak of the SON layer is ~5 μm under the anode surface. The SON profile is asymmetrical, increasing relatively sharply at the side closer to the anode, reaching the maximum value and then tailing away deeper into the sample. This is expected, as the frozen-in field is generally believed to be formed between the externally injected hydrogenated species such as H^+ or H_3O^+ and those immobile negative ions left behind in the so-called depletion region after the mobile cations (e.g., Na^+) migrate towards to the cathode.[11] Under the assumption of a narrow line distribution for the injected hydrogenated species and a wider depletion region with approximately constant negative ion density N, the theoretical SON profile should abruptly reach its peak value and then decreases linearly deeper into the sample with a slope of eN/ε, where ε is the dielectric permittivity of the silica glass. The formed frozen-in field E acts on the intrinsic third-order susceptibility of the silica through the relation $\chi^{(2)}=3\chi^{(3)}E$ and generates the SON in the thermally poled silica. Therefore, in principle, the SON profile should resemble the profile of the frozen-in field. The experimental results present some proof to this SON forming mechanism, at least in trend.

Time evolution of the SON layer was also characterized. The SON peak positions relative to the anode edge for three different poling time intervals were measured and plotted in Fig. 4. The accuracy of this measurement depends on the perpendicularity of the SON layer relative to the normal of the specimen stage of the microscope. In the sample preparing process, care was taken to optimize perpendicularity. Assuming a maximum 10° of angle deviation of the SON layer from the normal of the specimen stage of the microscope and a 5 μm focusing into the sample, we estimated the maximum error to be 1 μm. It can be seen that the SON layer moves deeper into the sample with poling time. This may be due to the movement of the injected hydrogenated species such as H^+ or H_3O^+ in the poling process. These cations, although with much lower mobility than Na^+, could still move towards the cathode under the act of the strong electric field under the anode. Thus, the frozen-in electric field, formed between these hydrogenated species and the negative ions, shifts deeper into the silica, and the resultant SON layer follows the same trend.

In conclusion, we have characterized the second-order nonlinear layer in fused silica plates thermally poled at 280 °C and 3.5 kV for different time intervals with SH microscopy. For samples poled for 30 min, the nonlinear layer is found ~5 μm away from the anode edge and has an FWHM of ~7 μm. It is also found that the peak position of the SON layer moves deeper into the samples with poling time. This SH microscopy is nondestructive and presents the real measurement of the spatial distribution of the SON layer without any dependence on the origin of the SON layer.

[1] R. A. Myers, N. Mukherjee, and S. R. J. Brueck, Opt. Lett. **16**, 1732 (1991).
[2] P. G. Kazansky, L. Dong, and P. St. J. Russell, Opt. Lett. **19**, 701 (1994).
[3] D. Wong, W. Xu, S. Fleming, M. Janos, and K. M. Lo, Opt. Fiber Technol. **5**, 235 (1999).
[4] J. Arentoft, M. Kristensen, K. Pedersen, S. I. Bozhevolnyi, and P. Shi, Electron. Lett. **36**, 1635 (2000).
[5] T. G. Alley and S. R. J. Brueck, Opt. Lett. **23**, 1170 (1998).
[6] W. Margulis and F. Laurell, Opt. Lett. **21**, 1786 (1996).
[7] A. Kudlinski, Y. Quiquempois, M. Lelek, H. Zeghlache, and G. Martinelli, Appl. Phys. Lett. **83**, 3623 (2003).
[8] Y. Uesu, S. Kurimura, and Y. Yamamoto, Appl. Phys. Lett. **66**, 2165 (1995).
[9] V. Kirilyuk, A. Kirilyuk, and Th. Rasing, Appl. Phys. Lett. **70**, 2306 (1997).
[10] J. Beermann, S. I. Bozhevolnyi, K. Pedersen, and J. Fage-Pedersen, Opt. Commun. **221**, 295 (2003).
[11] T. G. Alley, S. R. J. Brueck, and R. A. Myers, J. Non-Cryst. Solids **242**, 165 (1998).

Downloaded 12 Dec 2004 to 129.78.64.101. Redistribution subject to AIP license or copyright, see http://apl.aip.org/apl/copyright.jsp